ACS Catalysis

Research Article

pubs.acs.org/acscatalysis

Environmental Transmission Electron Microscopy Study of the Origins of Anomalous Particle Size Distributions in Supported Metal Catalysts

Angelica D. Benavidez,[†] Libor Kovarik,[‡,§] Arda Genc,[∥] Nitin Agrawal,[§] Elin M. Larsson,[⊥] Thomas W. Hansen,*[,⊗] Ayman M. Karim,*[,§] and Abhaya K. Datye*[,†]

[†]Department of Chemical & Nuclear Engineering and Center for Microengineered Materials, MSC 01 1120, University of New Mexico, Albuquerque, New Mexico 87131-0001, United States

[‡]Environmental Molecular Sciences Laboratory and [§]Institute for Integrated Catalysis, Pacific Northwest National Laboratory, P.O. Box 999, Richland, Washington 99352, United States

[∥]FEI Company, USA NanoPort, 5350 NE Dawson Creek Drive, Hillsboro, Oregon 97124, United States

[⊥]Division of Chemical Physics, Department of Applied Physics, and Competence Center for Catalysis, Chalmers University of Technology, 412 96 Göteborg, Sweden

[⊗]Center for Electron Nanoscopy, Technical University of Denmark, DK-2800 Kgs. Lyngby, Denmark

Supporting Information

ABSTRACT: In this Environmental Transmission Electron Microscopy (ETEM) study we examined the growth patterns of uniform distributions of nanoparticles (NPs) using model catalysts. Pt/SiO_2 was heated at 550 °C in 560 Pa of O_2 while Pd/carbon was heated in vacuum at 500 °C and in 300 Pa of $5\%H_2$ in Argon at temperatures up to 600 °C. Individual NPs of Pd were tracked to determine the operative sintering mechanisms. We found anomalous growth of NPs occurred during the early stages of catalyst sintering wherein some particles started to grow significantly larger than the mean, resulting in a broadening of the particle size distribution (PSD). The abundance of the larger particles did not fit the log-normal distribution. We can rule out sample nonuniformity as a cause for the growth of these large particles, since images were recorded prior to heat treatments. The anomalous growth of these particles may help explain PSDs in heterogeneous catalysts which often show particles that are significantly larger than the mean, resulting in a long tail to the right. It has been suggested previously that particle migration and coalescence could be the likely cause for such broad size distributions. We did not detect any random migration of the NPs leading to coalescence. A directed migration process was seen to occur at elevated temperatures for Pd/carbon under H_2. This study shows that anomalous growth of NPs can occur under conditions where Ostwald ripening is the primary sintering mechanism.

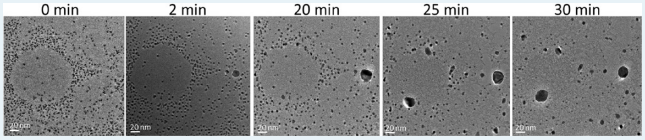

KEYWORDS: *catalyst sintering, Ostwald ripening, particle size distributions, Pt/SiO_2, Pd/carbon, environmental TEM*

INTRODUCTION

When heterogeneous catalysts are subjected to reaction environments at elevated temperatures there is a growth in particle size, and the particle size distributions (PSDs) usually show a long tail to the right, that is, particles that are significantly larger than the mean.[1−4] Some examples from previous work include the PSDs for Ni steam reforming catalysts aged at temperatures from 500 °C−750 °C,[2,4] for Pd automotive catalysts aged at 900 °C[3] and in Pd combustion catalysts aged at 1000 °C[1] all of whom show particles significantly larger than the mean, often 5−10 times larger. It is often speculated that particle migration (PM) could lead to coalescence and the formation of such large nanoparticles (NPs);[4,5] however, previous studies have concluded that only particles smaller than approximately 6 nm in size could likely show sufficient mobility to lead to coalescence.[6] There are only a few direct observations of particle mobility,[7] and recent work by scanning tunneling microscopy (STM) suggests that even particles smaller than 1 nm get pinned to the oxide surface and are rendered immobile.[8] On the other hand the largest particles observed in previous studies of industrial catalyst were of the order of 100 nm in diameter or even larger.[3,9] The origin of such large particles in industrially relevant catalysts aged at high temperatures is rather puzzling if PM is an unlikely mechanism for the growth of such large particles. The other accepted mechanism for particle growth is Ostwald ripening (OR), which involves interparticle transport of atomic species.

Special Issue: Operando and In Situ Studies of Catalysis

Received: July 30, 2012
Revised: September 26, 2012
Published: September 27, 2012

   dx.doi.org/10.1021/cs3005117 | *ACS Catal.* 2012, 2, 2349−2356

The classical mathematical model for OR predicts that the largest particles formed should only be 1.5 times as large as the mean size.[10] It was later suggested that a simple modification of the equations used to model OR could result in altered size distributions.[11] Some of these PSDs resulting from the OR formalism also resemble the log-normal distribution.[12] It is therefore of interest to determine if the larger particles seen in the experimentally determined PSDs are consistent with the models proposed in the literature.[11,12] The formation of abnormally large particles in industrial catalysts has major economic consequences since large particles consume a lot of the precious metal in a catalyst but provide very little reactivity. Most of the surface area in a catalyst comes from small particles, which have high surface area per unit of mass. To achieve the desired level of long-term performance and overcome the loss of metal surface area by sintering, catalyst manufacturers often resort to increased loading of the precious metal in industrial catalysts. With increasing cost of precious metals like Pt and Pd, there is a need to improve our understanding of growth patterns for NPs in supported catalysts.

One complication when working with catalysts prepared on an industrial scale is the uniformity of the initial catalyst precursor. It has been speculated that the large particles observed in the industrial catalysts could arise from non uniform distributions of the catalyst precursor. This initial distribution of precursor could result in locally high concentrations of metal in certain regions of the catalyst, and lead to abnormally large particles after catalyst aging. In industrial catalysts, it is difficult to image via microscopy the same region of a catalyst before and after long-term treatment. Therefore many studies have used model catalysts that start out with a uniform distribution of metal particles. The published PSDs when model catalysts were heated to elevated temperature also show the presence of anomalously large particles. For example, in their comprehensive review of supported metal catalysts, Wynblatt and Gjostein[10] report that anomalously large particles were seen in a model catalyst system consisting of Pt particles on a microcrystalline γ-Al_2O_3 film (100 Å thick). These authors proposed that the growth of the metal particles was related to evaporation of Pt in an O_2 containing atmosphere leading to volatile PtO_2 as the mobile species. Their observations were done at 700−1000 °C in a quartz tube with either air or 2% O_2 in N_2 at atmospheric pressure. It was found that higher O_2 partial pressure led to faster particle growth, and they attributed the abnormally large particles to a morphological instability whose details were not elucidated in their experiments. They speculated that there was a change in growth mode resulting from differences in the structure of the particles. "Normal" growth patterns for the first 7 h of sintering were followed by "abnormal growth" resulting in some particles growing considerable faster than average.[13] The abnormal growth rates led to an inflection point in a plot of mean radius as a function of time, but the precise location of the inflection depended on temperature and oxygen partial pressure. The growth patterns were modeled using power law growth models with different values of the exponent but without any mechanistic insight.[14] The emergence of the anomalously large particles could not be explained, but the authors did speculate that the particles that started to grow large were initially twinned particles whereas all other particles were single crystals.

Harris et al.[15,16] observed similar phenomena (growth of abnormally large particles) on model samples of Pt/Al_2O_3 heated to 600 °C−700 °C in air at atmospheric pressure for up to 8 h. Like the previous work by Wynblatt and Gjostein,[10] Harris et al.[15,16] also concluded that the abnormal growth patterns appeared at the later stages of catalyst sintering. The large particles that resulted were often observed to be highly faceted with hexagonal or triangular outlines. The authors conjectured that small particles would sinter via PM while larger particles would be virtually immobile and grow only via OR.[6] Hence, they argued that the phenomenon of abnormal growth was difficult to explain by PM and suggested that twinning of some particles might cause the generation of reentrant surfaces facilitating growth by interparticle transport. Since Pt is known to form a volatile oxide PtO_2, it is possible that vapor phase processes may also play a role. However, observations of abnormal growth are not confined only to Pt catalysts under oxidizing conditions since similar observations were reported for Ni/SiO_2 heated in H_2 and N_2 at temperatures ranging from 500 to 800 °C.[17] The data was fit to a power law, and it was inferred that the drastic changes in the fitting exponent indicated a change in mechanism from PM to OR. The PSDs show anomalously large particles in the sample sintered at 800 °C. Kim and Ihm[18] observed similar anomalously large particles for a Ni/Al_2O_3 model catalyst system after heating to 800 °C in H_2 atmosphere for 43 h.

The literature on catalyst sintering shows that the mechanism of the formation of large particles, and the long tail in the PSD, is still poorly understood. There is uncertainty about the importance of PM versus OR as mechanisms responsible for the growth of metal particles. With recent advancements in the technique of in situ transmission electron microscopy (TEM), it is now possible to study smaller particles (which would be more likely to undergo PM) and to expose the catalyst to oxidizing as well as reducing atmospheres in the microscope. We decided to explore the growth patterns of Pt and Pd NPs that were most likely to undergo PM (by using noninteracting supports such as silica and carbon). Pt was studied under oxidizing conditions and Pd was studied under reducing conditions. NPs were prepared by evaporation of metal, or via colloidal routes (leading to weak interactions with the support). Continuous observations of Pd allowed us to infer the mechanisms of particle growth. Since the samples were examined before and after heat treatment, we ensured that there were no locally high concentrations of metal that could lead to anomalous growth patterns. The term locally high concentrations is meant to indicate the type of nonuniformities seen in supported catalysts where excess catalyst precursor may lead to higher coverage of the metal in some parts of the catalyst sample. The specific objectives of this work were to determine if abnormal growth patterns were prevalent in the early stages of catalyst sintering and whether the origins of the formation of larger particles could be identified. A secondary objective was to determine the mechanism of particle growth and its influence on the formation of a long tail in the PSD. The surprising observation in this work is that abnormally large particles could be observed even under conditions where the particle growth occurred exclusively through interparticle transport of atomic species via OR, and that PM did not occur, even with the particles that were most weakly held on the support.

dx.doi.org/10.1021/cs3005117 | ACS Catal. 2012, 2, 2349−2356

EXPERIMENTAL SECTION

Pt NPs. The model catalyst samples were prepared by depositing 10 nm SiO_2 using reactive sputtering (FHR MS150) on Si_3N_4 supported on 0.35 mm thick Si wafers followed by deposition of Pt (99.99% nominal purity, Nordic High Vacuum AB) using a AVAC HVC600 electron beam evaporator operated at a base pressure of 4×10^{-6}. The samples were mounted in a Gatan 652 double tilt heating holder with an Inconel furnace. In situ Environmental Transmission Electron Microscopy (ETEM) experiments were carried out in a FEI Titan ETEM equipped with a differential pumping system.[19] After insertion of the sample, O_2 gas was allowed to flow in using a digital mass flow controller at 4 N mL/min. This flow resulted in a pressure in the sample chamber of 560 Pa. After the pressure had stabilized, the temperature was gradually increased to 550 °C over a period of about 10 min. After an additional 30 min allowing for stabilization of the sample, a set of images was acquired. This image set will be referred to as t = 0. Subsequent image sets were acquired after 3, 5.5, 8, and 10 h respectively. The images were acquired with a current density of about 2A/cm^2 with 0.5 s exposure time. Each image set was acquired at a new location to minimize the effects of the electron beam. Each location was exposed for a maximum of 5−10 s prior to image acquisition. After image acquisition the sample was rapidly moved several micrometers to capture a new region to minimize total electron beam exposure. Images were analyzed by applying a low-pass filter to minimize high frequency noise in the images and were subsequently segmented on contrast, and mean particle sizes were automatically determined. The results of automated counting were compared with manual counting to ensure there were no artifacts. More than 2500 particles were included in each set. Each image set consists of 5−8 images, and the mean diameter from each image allowed us to derive the standard error of the mean, and a confidence interval.

Pd NPs. The Pd NPs were synthesized by the reduction of Pd acetate with methanol based on the approach described by Burton et al.[20] Specifically, 11.2 mg of Pd acetate (Sigma-Aldrich, recrystallized in the lab using glacial acetic acid) was dissolved in 1 mL of anhydrous toluene (Sigma-Aldrich) followed by the addition of 16.4 μL of oleylamine (1:1 oleyalmine:Pd, molar ratio) used as the capping agent. The solution was degassed using ultra high purity Ar (20 mL/min) for 20 min to remove any dissolved O_2. Similarly, anhydrous methanol (Sigma-Aldrich) was also degassed and then added to the Pd acetate/oleylamine in toluene solution at 1:1 v:v ratio to get a final concentration of 25 mM Pd acetate. The Pd was reduced by heating the solution at 60 °C (under a stagnant Ar atmosphere) on a hot plate for 30 min. The solution color changed from dark yellow to black. This method allowed us to create a stable suspension of Pd NPs with a mean diameter of 3 nm. The colloidal solution was diluted 200:1 with toluene, and a drop of the diluted solution was deposited on a Protochips Aduro TEM holder. The Aduro heating holder consists of a carbon film deposited on a Si MEMS device that can be heated rapidly via resistive heating. The sample was mounted in aberration corrected FEI Titan ETEM G2, and all imaging was performed at the accelerating voltage of 300 kV, and reduced electron dose rate of approximately 0.15−0.3 A/cm^2 to minimize electron beam induced effects. Under the imaging conditions used, there was no change in the size or distribution of NPs at room temperature. To further minimize the electron beam induced effects, the beam was blanked during prolonged experiments, and the majority of the observations reported here occurred in an "interrupted heating cycle" mode. That is, the observations were made at room temperature after the sample was heated to or above 500 °C for a preset period of time. Because of the rapid heating/cooling rates and very low drift rates associated with the Aduro heating holder, observations of multiple areas of interest could be performed almost instantly. The temperature of 500 °C was chosen since it represents the approximate onset of sintering for Pd NPs. The majority of the experiments were performed in vacuum at the base pressure of ~10^{-5} Pascal, one additional set of experiments involved heating the sample in 5%H_2 in Argon at the pressure of approximately 300 Pa.

RESULTS

Aging of Pt/SiO_2 in O_2. The experiment commenced by acquiring several images from the sample after it had stabilized at the operating temperature of 550 °C, after which the beam was switched off. The sample was left in the microscope at elevated temperature till it was time to acquire the next set of images. In this manner, any given region of the specimen was exposed to the electron beam for a very short time to perform the imaging. This process was continued for a total of 10 h of exposure at 550 °C, with the images being acquired in areas that were randomly determined so that any one region was only exposed to the beam for 5 s. Figure 1 shows the PSDs after 0, 3, 5.5, 8, and 10 h respectively after heating to 550 °C in 560 Pa O_2. The PSDs were derived from images that were acquired at a high magnification with a field of view of 125 × 125 nm^2 (Figure 2a and 2b). These images show very little change in the average size. However, one of the particles seems to have grown larger than the average. When images were acquired at medium magnification, Figure 2c and 2d (field of view 550 × 550 nm^2), it became clear that this phenomenon was quite widespread across the entire sample and that several of the particles had grown larger than the average, indicating an anomalous growth pattern. The figure illustrates that the sintering of platinum particles under these conditions is a slow process and very little

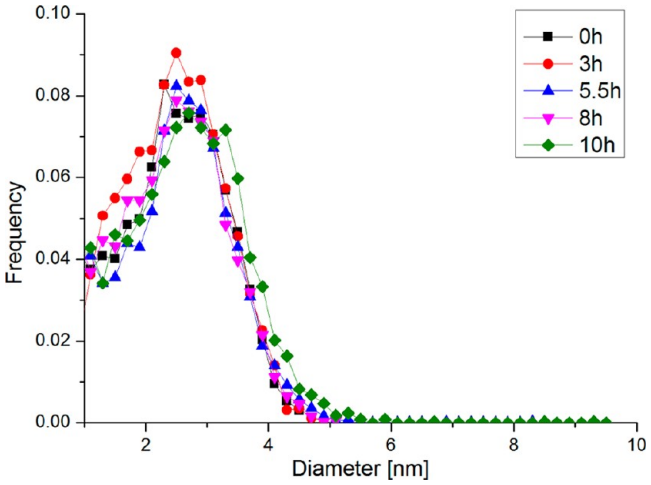

Figure 1. PSDs determined after 0, 3, 5.5, 8, and 10 h respectively from images acquired at high magnification as shown in Figure 2 images a and b. The distributions appear very similar up to 8 h after which a slight shift to larger particles is observed. The bin size is 0.2 nm.

dx.doi.org/10.1021/cs3005117 | ACS Catal. 2012, 2, 2349−2356

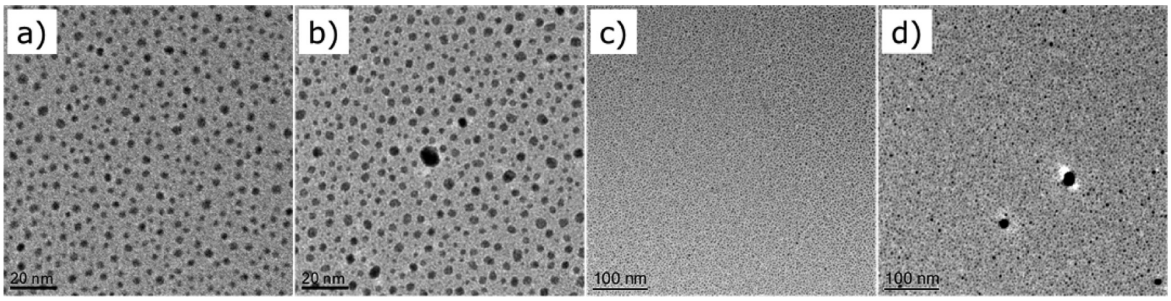

Figure 2. Platinum NPs supported on SiO_2/Si_3N_4 acquired in 560 Pa O_2 at 550 °C. Panels (a) and (b) are acquired after 30 min and panels (c) and (d) after 10 h. Panels (a) and (b) show high magnification images recorded after 30 min and 10 h respectively and used for determination of PSDs. Panels (c) and (d) show medium magnification images recorded after the same times. At medium magnification, panels (c) and (d), a larger field of view is captured and the appearance of anomalously large particles is evident. Supporting Information, Figure S10 shows a low magnification view with even more larger particles visible.

change is observed. After 10 h, a slight shift of the distribution to larger particles is observed. Table 1 shows the particle density for this sample as a function of aging time. The table shows the average number of particles per unit area and the standard error of the mean particle concentration. Since the error varies from one image set to another, we used a pooled estimate of the standard error (0.1×10^4) to derive the 95% confidence interval for the mean. With a confidence interval of $\pm 0.2 \times 10^4$, we conclude that sample aged for 10 h has a lower average particle density than the other samples. Since we did not observe a given region of the sample, we cannot directly infer the operating sintering mechanism. However, we note that there is no change in particle concentration in the vicinity of the larger particles in Figures 2b and 2d. If the growth occurred via particle coalescence, we would have expected to see a depletion zone, where particles disappeared because of coalescence. Hence we infer that the dominant sintering mechanism must be OR. Under the strongly oxidizing conditions applied in the microscope, the formation of a volatile platinum oxide is possible. This platinum oxide can serve as the mobile species for transporting Pt species from one particle to another. The results show that anomalous growth of NPs can commence at the very early stages of catalyst sintering. Similar observations were made with the Pd/carbon system as described in the next section.

Table 1. Particle Concentration Per Unit Area Derived from Pt/SiO_2 Samples Aged at 550 °C in 560 Pa O_2[a]

aging time	number of images	total number of particles counted	average number of particles per unit area	standard error of the mean
hours	n	#	#/sq. micrometer	s/sqrt(n)
0	8	3992	3.23×10^4	0.14×10^4
3	5	2565	3.26×10^4	0.07×10^4
5.5	7	4214	3.77×10^4	0.09×10^4
8	6	3218	3.31×10^4	0.16×10^4
10	7	3364	2.92×10^4	0.04×10^4

[a]For each treatment time, the standard deviation (s) is computed from the variance of the mean value recorded for each image.

Aging of Pd/Carbon in Vacuum. Figure 3 shows images after 0, 2, 20, 25, and 30 min, respectively, after heating to 500 °C in vacuum. The figure illustrates the growth of palladium particles under these conditions. By carefully monitoring the positions of the particles, it was concluded that there was very little movement of the particles. What is most striking is the growth of a few anomalously large particles. Before the heat treatments (0 min), the regions where anomalous growth was observed do not show particularly high density of particles and instead have a fairly uniform distribution of similarly sized particles. In Figure 3 (0 min), 853 particles were counted. The number of particles in this region decreased with time and 234 particles remained after 30 min of heating. Figure 4 shows the PSDs corresponding to the images in Figure 3. Initially, there is a narrow PSD that shifts slightly to the right after 2 min of heating. After 20 min of heating, the size distribution turns bimodal and there is an increase in the number of smaller particles that were not observed earlier. This is clear evidence that the primary sintering mechanism is OR and not coalescence. The bimodal size distribution becomes more prominent after 25 min of heating and then becomes less noticeable after 30 min of heating. Figure 5b and 5d show the same region of the sample imaged in Figure 3 after 2 and 20 min of heating, respectively. A region of this image was

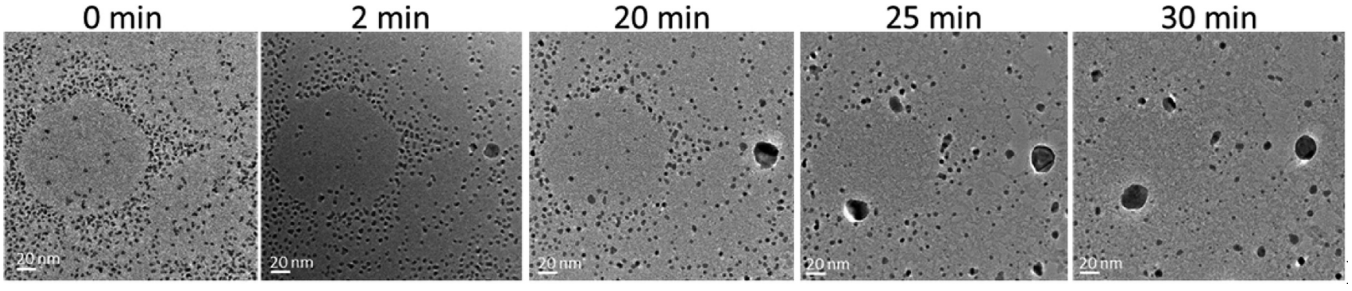

Figure 3. Palladium NPs supported on a carbon film imaged in vacuum at 500 °C. The images were acquired after 0, 2, 20, 25, and 30 min of heating, respectively. The series of images capture the anomalous growth of large particles.

dx.doi.org/10.1021/cs3005117 | ACS Catal. 2012, 2, 2349−2356

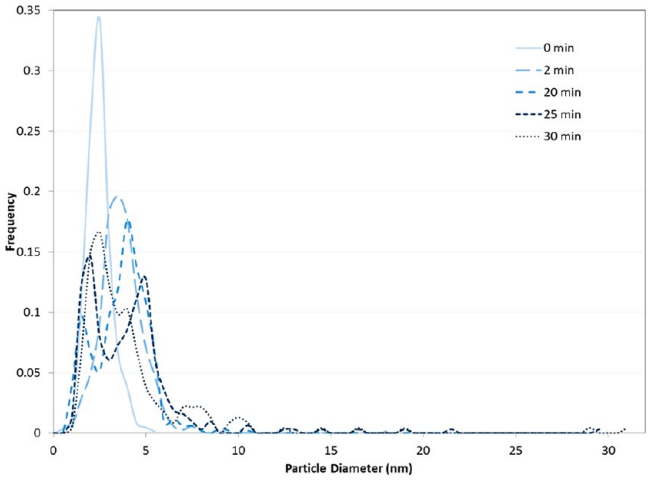

Figure 4. PSDs corresponding to images in Figure 3. The distributions show an appearance of particle size bimodality after heating Pd NPs at 500 °C in vacuum. The bin size is 0.5 nm.

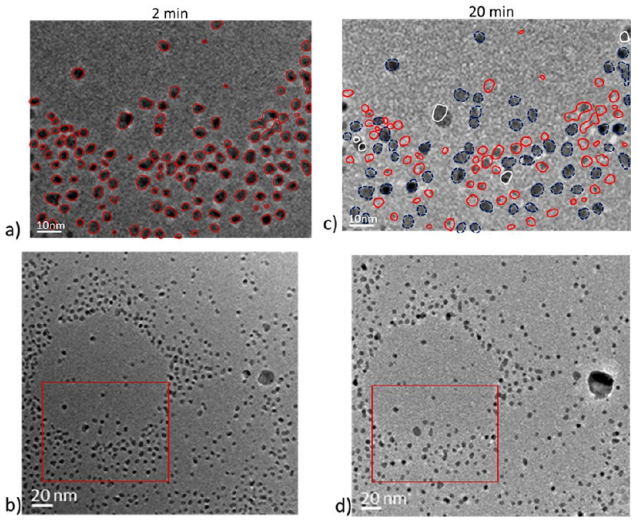

Figure 5. Images (b) and (d) correspond to images in Figure 3 after 2 and 20 min of heating, respectively. Images (a) and (c) are higher magnifications of the areas shown in the red boxes. An outline of the particles in image (a) is shown in red. This mask was transferred to image (c) to show how these particles changed over time. The outline is changed to white where particles grew and to blue where particles had no change. The outline remained red for particles that shrunk or disappeared.

magnified and is shown as Figure 5a and 5c. In Figure 5a each particle is outlined in red to identify its position and size. The lines marking all the particles were converted into a mask, which was transferred to Figure 5c to see clearly the changes that occur after heating the sample. Where the particles grew in size, the mask color was changed to white, and where the particles decreased in size or disappeared, the mask color was retained and is shown in red. The mask color was changed to blue for particles that had little or no apparent change. This makes it easy to see that while there are changes in size, none of the particles have moved. In addition to the particles being immobile, some particles are increasing in size and there are many particles that have shrunk in size; hence, the mechanism is clearly OR. This figure also illustrates that the particles that are growing in size are in the immediate vicinity of particles that are neither migrating nor shrinking in size. The same sample region was further observed for 10 more minutes as shown in Figure 6. Here a new mask is generated for each image so as to

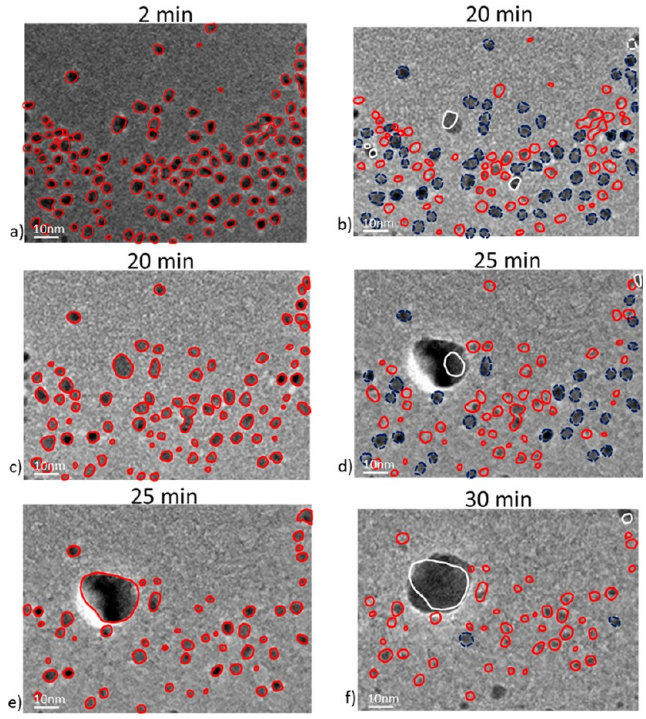

Figure 6. Images of the continued evolution of the region shown in Figure 5. Images on the left have a mask outlining the particles. Each mask was transferred to the image to its right, which is the next image in the time series. The outline is changed to white where particles grew and to blue where particles had no change. The outline remained red for particles that shrunk or disappeared. The anomalous growth of one particle can clearly be seen.

show incremental changes. The particles that started to grow larger than their neighbors in the early stages continued to grow in size until they were about 10 times the mean diameter.

The phenomena documented here were confirmed to occur in other regions of the sample. Two sets of images from different regions of the sample (regions A-B, Figures S1–S6) have been included in the Supporting Information. These images show that anomalous growth patterns similar to those documented in Figures 3–6 occurred elsewhere on this sample. At the end of the heating cycle, sample areas that were not observed at earlier times in the heat treatment sequence were imaged. The overall appearance of the sample in regions not imaged previously (and hence not exposed to the electron beam) was similar to the regions that were repeatedly observed at successive time intervals. Such an image is shown in Supporting Information, Figure S8 where anomalous growth of particles is seen after 30 min of aging in vacuum. Heating the specimen in vacuum for 30 min causes some degradation of the carbon film which can be seen in Supporting Information, Figure S8. The region that was repeatedly exposed to the electron beam for 30 min also showed similar changes; see Figures 3, 6, and Supporting Information, Figure S6. The carbon film is starting to disintegrate and shows regions of lighter contrast. We expect that the traces of oxygen and moisture may cause gasification of the carbon. Electron beam exposure may create point defects and further accelerate this oxidation of the carbon film. We did not see any influence of

dx.doi.org/10.1021/cs3005117 | ACS Catal. 2012, 2, 2349–2356

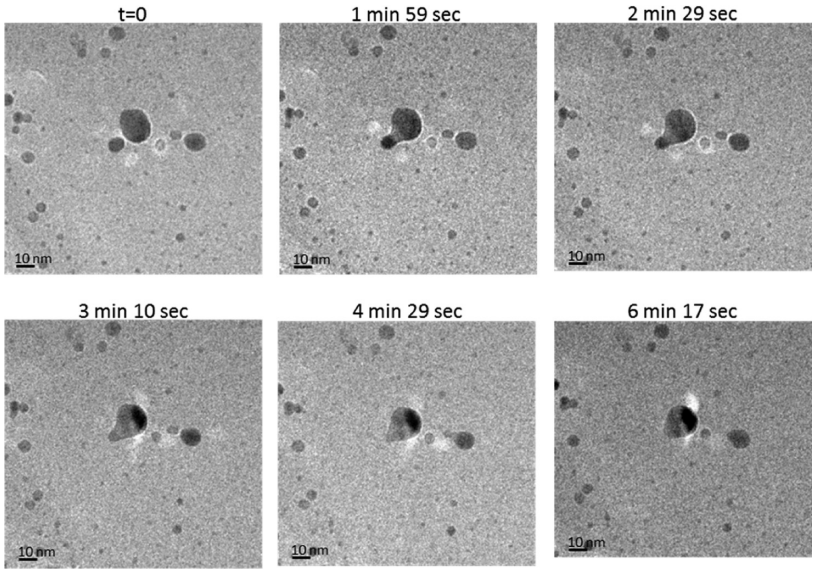

Figure 7. Images of a time series of the same region of Palladium NPs on a carbon film heated to 600 °C in 5%H_2/Ar. The images show the formation of a neck between two large adjacent particles and their eventual coalescence after more than 6 min. The process of particle fusion is clearly seen in movie 1 included in the Supporting Information.

the electron beam on the phenomenon of OR at the beam illuminations used in these experiments. To investigate the role of the electron beam on the metal particles, additional experiments were performed at higher beam doses as described later.

Aging of Pd/Carbon in H_2. A second sample of the Pd/carbon was heated in H_2 to study the role of the gas phase environment. This sample was first heated in vacuum at 500 °C, and anomalous growth patterns were observed that were similar to those described in the previous section. The sample was cooled down and exposed to flowing H_2 at a pressure of 300 Pa (5% H_2 in Argon). Next the sample was heated to 500 °C and no further changes in size over the time frame of our observation were found to occur because of the presence of H_2. The major changes had already occurred during the heating of the sample in vacuum to 500 °C. The sample was then heated to 600 °C in the H_2 atmosphere and more rapid transformations in the Pd NPs occurred. One such sequence is shown in Figure 7 where adjacent particles form a neck and eventually merge to form a single large particle. A movie documenting the evolution of this region is included in the Supporting Information (movie 1). The movie shows clearly that the process of neck formation and that the fusion of two particles is driven by atomic scale migration events. The process repeats itself with two smaller particles adjacent to the large particle in the center of the image. It appears that when particles are in close proximity, they appear to move close to each other and coalesce. The actual process of merging of the particles occurs first by the formation of a neck or bridge, which then fills in via metal atoms migrating to the reentrant surface. The process of coalescence observed at 600 °C in H_2 is very similar to that reported by Yang et al.[21] who called it attractive migration and coalescence. This process is caused by the non uniform surface concentration of metal atoms around the NPs. The movie sequence shows clearly that the fusion of these particles is not caused by random migration of the metal particles, rather a directed motion is seen to occur causing the neck formation and eventual fusion of the particles. Further work is needed to investigate the role of gas atmosphere and temperature on the onset of particle fusion.

Electron Beam Effects on NP Stability and Mobility. To investigate the role of the electron beam, the Pt samples were examined at higher beam doses that would typically be used for high resolution TEM imaging. The sample was uniformly illuminated for an extended period of time with a beam current density of 5A/cm^2, and image sequences were acquired with an exposure time of 0.5 s for each image. A movie showing the evolution of this sample under high beam dose conditions is included in the Supporting Information (movie 2). Two effects were observed in the case of the Pt sample, loss of Pt because of evaporation and random migration of the Pt particles leading to coalescence. Both these effects were seen on the silica films, and less so on carbon substrates. Still images from this experiment are also included in the Supporting Information (Figure S9). Here, a dramatic decrease in the number of Pt particles in a given region was observed. A similar effect of the electron beam was also noticed by Simonsen et al.[22] where Pt particles were lost because of evaporation under intense electron irradiation. The reason for this could be the increased interaction of the primary electrons with the thick substrate resulting in local heating and the formation of a volatile PtO_2. Increased mobility of the NPs on the silica substrates was also observed, leading to migration and coalescence at high beam doses.[22] However, experiments with Ni/$MgAl_2O_4$ supports at high temperatures[23] did not show any enhanced mobility of NPs because of electron beam exposure. It appears that the particle mobility seen at elevated temperatures on model thin film supports is not necessarily seen on conventional high surface area catalyst supports and is a phenomenon that deserves further study to establish the validity of these model catalysts.

It is therefore evident from the image sequence and the movies included in the Supporting Information (movie 2 and Figure S9) that care has to be taken when observing NPs in TEM, especially in a gaseous atmosphere as found in an ETEM. Several phenomena can occur that are unique to the ETEM environment. The interaction of the high energy primary

dx.doi.org/10.1021/cs3005117 | ACS Catal. 2012, 2, 2349−2356

electrons and the gas molecules causes ionization providing a much more reactive atmosphere than that found in a catalytic reactor. Furthermore, surface atoms can be sputtered off the surface of the NPs. The only way around this problem is to minimize the electron dose rate on the particles, and to reduce the exposure time. This can be done either by minimizing the current density or by minimizing the time to which the NPs are exposed to the electron beam as shown recently by Kawauchi et al.[24] Since low magnification imaging could be used to obtain the PSDs presented here, and a perfect focus was not necessary, it was possible to perform the focusing on sample regions adjacent to those of interest. In this manner the regions of the sample imaged received electron exposure for less than 5−10 s. This method allowed recording of images with an acceptable signal-to-noise ratio for measuring the particle diameters. We note that a systematic investigation of beam effects was perfomed by Simonsen et al.[22] who concluded that for Pt/SiO_2 a beam current of $1A/cm^2$ would cause a decrease in particle diameter of 0.15 nm/min. Extrapolating to our beam dose of 2 A/cm^2 we would expect that over the 10 s of total exposure, we can expect a decrease in particle size of 0.05 nm which would be undetectable at the low magnifications we used. We did perform extended imaging at our beam current of $2A/cm^2$ and did not observe any noticeable changes in sample morphology. Only at the higher beam dose of $5A/cm^2$ did we see noticeable changes which are described in the Supporting Information (movie 2 and Figure S9). A more sensitive camera would allow us to further reduce the beam dose. There is currently an interest in utilizing direct electron detection inspired by the soft-matter community. Such cameras would be an asset to the materials science community, especially for the study of catalysts under working conditions.

For the Pd/C sample, we examined regions not exposed to the electron beam during the heat treatment. We found that the results were very similar to those found in regions that were repeatedly examined over the course of the heat treatment. Supporting Information, Figure S8 shows an example of a region heated at 500 °C for 30 min. The sample morphology is very similar to those regions that were observed multiple times (Figures 3, 6, Supporting Information, Figures S5 and S6), and similar anomalous growth of Pd NPs was seen in each of these images.

DISCUSSION

The model samples presented here are considerably different from the real-world catalysts used in industry, but they provide suitable systems for determining PSDs. The samples are uniformly thick, and there are no overlapping support features. The carbon and silica substrates have a smooth texture, and there is no surface topography or heterogeneity for anchoring metal atoms or NPs. The HAADF images of the carbon and the silica films confirm the uniformity of sample thickness. Industrial catalyst supports consist of spheroidal particles with surface curvature and reentrant surfaces. Crystalline supports such as alumina expose surface facets, and the industrial supports have a much higher degree of surface roughness. The model catalysts are therefore ideal substrates to study the role of PM on the sintering of NPs. Furthermore, the same region of the specimen can be observed before and after heat treatment, allowing us to infer mechanistic details. Prior to heat treatments, it was confirmed that the distribution of the metal particles was uniform. This ensures that the observed PSDs after heat treatments were not influenced by the initial nonuniformities in the samples as-prepared.

Two different metals were studied: Pt on silica and Pd on carbon. The Pt sample was heated in O_2 and the Pd sample in H_2. The Pd/carbon sample was also studied in vacuum to determine the behavior of the metal without the presence of the gas phase. Our observations show that the metal particles are effectively immobile on either sample, independent of the gas phase, at a temperature of 500 °C. Anomalous growth was evident in each of the samples, wherein some particles start to grow larger than the mean, and continue to do so until they reach sizes as large as 10 times the mean diameter. These particles start to grow in regions that are otherwise no different from their neighbors. However, as some particles grow in size, others shrink or disappear indicating that the process can be explained by atomic scale migration of mobile species emitted from the NPs, that is, OR. The classical model for OR would predict a sharp cut off at 1.5 times the mean diameter.[10] The modified equations developed more recently suggest that a log-normal distribution may also be possible during OR, based on the formalism of the mean field approximation and a linearization of the Gibbs−Thompson equation for surface energy.[11,12] Both of these assumptions have been questioned in the context of OR.[25,26] Nonetheless we examined carefully whether the larger particles we observed could be consistent with a log-normal distribution. The results are presented in the Supporting Information, Figures S10−S13 and Tables S1−S3. In each of the observed images, we found that the abundance of the larger particles far exceeds what would be expected from a log-normal distribution. Therefore we conclude that the growth of isolated particles as seen in this work would not be predicted by the classical mean field theory of OR.

The anomalous growth of particles was seen at 500 °C for Pd/carbon where no coalescence of particles was detected. We did observe the fusion of neighboring particles when the Pd/carbon sample was heated to 600 °C in H_2. In this case, coalescence was initiated by neck formation, and the particles appeared to move closer to each other prior to neck formation. Such directed motion has been suggested to occur because of growth-decay flow of the island edges driven by nonuniform surface concentration around the islands.[21] Images of particles undergoing coalescence (see Figure 7) could be misinterpreted as resulting from PM, but no random migration of individual particles prior to the onset of coalescence was observed, as can be seen from the movie (Supporting Information, movie 1) of the sample undergoing the fusion process. All of the particle motion was directed motion toward each other when the particles were in close proximity. The results presented here do not fully explain the anomalous growth of NPs, since it was not possible to discern the features that are responsible for this growth pattern. But we can conclude that the process occurs because of migration of atomic species and not because of coalescence of NPs. Further study is needed to fully elucidate this anomalous growth phenomenon which may be responsible for the long tail in the PSD generally seen in heterogeneous catalysts. Factors that need to be considered are the heterogeneity of real catalyst supports and the role of the gas phase and adsorbates. Abnormal grain growth has also been studied in the field of metallurgy which may provide clues to operative mechanisms.[27]

This study helps elucidate a phenomenon of great importance to heterogeneous catalysis, the growth of NPs at elevated temperatures. By using model catalysts, we are able to

study the evolution of individual NPs and identify the mechanisms of catalyst sintering. Under our conditions, OR is the dominant mechanism, and we did not detect any random migration of NPs leading to coalescence. During OR we found anomalous growth patterns that result in some particles growing much faster than their neighbors. The frequency of occurrence of these larger particles does not fit the log-normal distribution at short sintering times.

CONCLUSIONS

An ETEM study of Pd/carbon was performed by continuous observation of individual NPs when the catalyst was heated to 500 °C and above. We also studied Pt/SiO_2 that was heated in the microscope to 550 °C in O_2, but we did not perform continuous imaging of the same region of the sample in this case. Anomalous growth patterns were detected wherein some particles started to grow much larger than their neighbors. The anomalous growth patterns were not caused by migration and coalescence of particles. Rather, we found that coalescence occurred only at elevated temperatures and only when particles were in close proximity. No random migration of particles was detected; the only movement was a directed motion where neighboring particles were attracted to each other leading to neck formation and fusion. The dominant process leading to particle growth was OR. The anomalous growth of NPs cannot be predicted by a mean field theory and must take into account local particle concentrations and the structure of individual NPs. These anomalous growth patterns observed may help explain the long tail in the PSDs observed in heterogeneous catalysts. However, we were not able to discern any features that could help us predict which particles would show the anomalous growth patterns, since they occurred in regions which looked very similar to the rest of the sample. We can, however, rule out nonuniform metal loading, or a high concentration of NPs in close proximity, as factors responsible for anomalous growth.

ASSOCIATED CONTENT

Supporting Information

Images, movies, and PSDs. This material is available free of charge via the Internet at http://pubs.acs.org.

AUTHOR INFORMATION

Corresponding Author

*E-mail: datye@unm.edu (A.K.D.), thomas.w.hansen@cen.dtu.dk (T.W.H.), Ayman.Karim@pnnl.gov (A.M.K).

Funding

The research described in this paper was supported, in part, by the Chemical Imaging Initiative at Pacific Northwest National Laboratory (PNNL). It was conducted under the Laboratory Directed Research and Development Program at PNNL, a multi program national laboratory operated by Battelle for the U.S. Department of Energy. A.D.B. acknowledges the National Science Foundation's GRFP under NSF Grant DGE-0237002 G. A.K.D. and A.D.B. acknowledge financial support from NSF Grant OISE 0730277, DOE Grant DE-FG02-05ER15712, and a contract from PNNL through the Chemical Imaging Initiative. The A. P. Møller and Chastine Mc-Kinney Møller Foundation is gratefully acknowledged for its contribution towards the establishment of the Center for Electron Nanoscopy in the Technical University of Denmark where the Pt ETEM experiments were performed. The Pd ETEM experiments were performed at the Environmental Molecular Sciences Laboratory (EMSL), a user facility operated by the DOE at PNNL.

Notes

The authors declare no competing financial interest.

ACKNOWLEDGMENTS

The authors thank Dr. Sergei Ivanov and Aaron Jenkins for providing recrystallized Pd acetate and for helpful discussion and comments.

REFERENCES

(1) McCarty, J. G.; Malukhin, G.; Poojary, D. M.; Datye, A. K.; Xu, Q. *J. Phys. Chem. B* **2005**, *109* (6), 2387−2391.
(2) Sehested, J.; Carlsson, A.; Janssens, T. V. W.; Hansen, P. L.; Datye, A. K. *J. Catal.* **2001**, *197* (1), 200−209.
(3) Xu, Q.; Kharas, K. C.; Croley, B. J.; Datye, A. K. *ChemCatChem* **2011**, *3* (6), 1004−1014.
(4) Baker, R. T. K. *Catal. Rev.- Sci. Eng.* **1979**, *19* (2), 161.
(5) Granqvist, C. G.; Buhrman, R. A. *J. Catal.* **1976**, *42*, 477−479.
(6) Harris, P. J. F. *Int. Mater. Rev.* **1995**, *40* (3), 97−115.
(7) Baker, R. T. K.; Harris, P. S.; Thomas, R. B. *Surf. Sci.* **1974**, *46* (1), 311−316.
(8) Sanders, L. M. Ph.D. Thesis, University of New Mexico, Albuquerque, NM, 2003; http://search.proquest.com/advanced.
(9) Datye, A. K.; Xu, Q.; Kharas, K. C.; McCarty, J. M. *Catal. Today* **2006**, *111* (1−2), 59−67.
(10) Wynblatt, P.; Gjostein, N. A. *Prog. Solid State Chem.* **1975**, *9*, 21−58.
(11) Coughlan, S. D.; Fortes, M. A. *Scr. Metall. Mater.* **1993**, *28* (12), 1471−1476.
(12) Fuentes, G. A.; Salinas-Rodriguez, E. Realistic particle size distributions during sintering by Ostwald ripening. In *Catalyst Deactivation 2001, Proceedings*; Spivey, J. J., Roberts, G. W., Davis, B. H., Eds.; Elsevier Science Bv: Amsterdam, The Netherlands, 2001; Vol. *139*, pp 503−510.
(13) Wynblatt, P. *Acta Metall.* **1976**, *24*, 1175−1182.
(14) Wynblatt, P.; Betta, R. A. D.; Gjostein, N. A. Particle Growth in Supported Catalysts. In *The Physical Basis for Heterogeneous Catalysis*; Drauglis, E.; Jaffee, R. I., Eds.; Plenum Press: New York, **1975**; p 501.
(15) Harris, P. J. F.; Boyes, E. D.; Cairns, J. A. *J. Catal.* **1983**, *82* (1), 127−146.
(16) Harris, P. J. F. *J. Catal.* **1986**, *97* (2), 527−542.
(17) Kuo, H. K.; Ganesan, P.; De Angelis, R. J. *J. Catal.* **1980**, *64* (2), 303−319.
(18) Kim, K. T.; Ihm, S. K. *J. Catal.* **1985**, *96* (1), 12−22.
(19) Hansen, T. W.; Wagner, J. B.; Dunin-Borkowski, R. E. *Mater. Sci. Technol.* **2010**, *26* (11), 1338−1344.
(20) Burton, P. D.; Boyle, T. J.; Datye, A. K. *J. Catal.* **2011**, *280* (2), 145−149.
(21) Yang, W. C.; Zeman, M.; Ade, H.; Nemanich, R. J. *Phys. Rev. Lett.* **2003**, *90* (13), 136102.
(22) Simonsen, S. B.; Chorkendorff, I.; Dahl, S.; Skoglundh, M.; Sehested, J.; Helveg, S. *J. Am. Chem. Soc.* **2010**, *132* (23), 7968−7975.
(23) Hansen, T. W., Ph.D. Thesis, Technical University of Denmark, Lyngby, Denmark, 2006; http://orbit.dtu.dk/services/downloadRegister/5100724/phdthesis_T_W_Hansen.pdf.
(24) Kuwauchi, Y.; Yoshida, H.; Akita, T.; Haruta, M.; Takeda, S. *Angew. Chem., Int. Ed.* **2012**, *51* (31), 7729−7733.
(25) Challa, S. R.; Delariva, A. T.; Hansen, T. W.; Helveg, S.; Sehested, J.; Hansen, P. L.; Garzon, F.; Datye, A. K. *J. Am. Chem. Soc.* **2011**, *133* (51), 20672−20675.
(26) Morgenstern, K.; Rosenfeld, G.; Comsa, G. *Surf. Sci.* **1999**, *441* (2−3), 289−300.
(27) Rollett, A. D.; Mullins, W. W. *Scr. Mater.* **1997**, *36* (9), 975−980.